University of Reading

Department of Mathematics

Abstract

This project was motivated by the needs of the oil industry for improved forecasts in the central Caspian Sea. Data for the months of August 2004 to January 2005 taken from an oil rig was provided by FUGRO GEOS. The

Declaration

I confirm that this is my own work, and the use of all material from other sources has been properly and fully acknowledged.

Richard Frühmann

Acknowledgement

I would like to thank Dr. Robert Plant for his supervision and guidance throughout this project. His open approach towards the project allowed for stimulating discussions and a plethora of ideas. I would also like t

Contents

Chapter 1

Introduction

Mountains and lakes are known to influence atmospheric flows on all scales ranging from turbulent eddies of a few hundred meters through to Rossby waves in the global circulation. [12] Often severe winds can be induced locally in a relatively sedate mean flow. Some are regular and highly predictable, such as sea breezes, while others appear without warning.

Local winds are highly dependent on the shape of the terrain and require a high resolution grid to be captured accurately by computer models. For remote locations - that is, remote from the Western world where computer models aid accurate forecasting - there rarely exists a high resolution grid. As a result, industries which operate in such locations often struggle to get reliable forecasts.

One such region are the oil fields in the central Caspian Sea. There high mountains, in particular the Caucasus, but also the lesser Caucasus and the Elbruz ranges, significantly modify synoptic scale flows in a very complex manner. Frequent strong winds result which hazard the drilling operations

Structure of the Report

To begin with it is important to investigate all the known mech

Chapter 2

Literature Review

2.1 General Literature

Lake Winds

Large bodies of water act as good thermal capacitors because overturning in the upper layers allows heat to be advected more effectively and to greater depths than through land surfaces. Temperature contrasts between the land and water surfaces are the result.

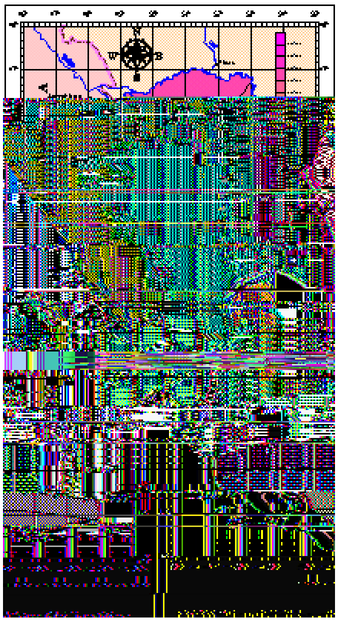

Figure 2.1: Distribution of annual mean wind strength. Image taken from Caspian Seafacts [21]

Abseron peninsula where they have an annual mean of 8-9 ms^{-1}. [21]

Due to its depth, the southern part of the lake acts as a thermal reservoir. This is seen by the mean cyclonic (anticyclonic) circulation in the winter (summer) seasons. The primary influence on the wind is through the orography which generates stationary inertial gravity and Rossby waves. [5] The dominant orographic feature in the central region are the Caucasus mountains which extend from the Black Sea to the Abseron peninsula.

Chapter 3

Data

The instable socio-economic situation in the Caspian Sea region has meant

3.1 Orography

The orography around the Abseron Peninsula is dominated by the high ridge

$C \quad AP \quad E \qquad DA \quad A$

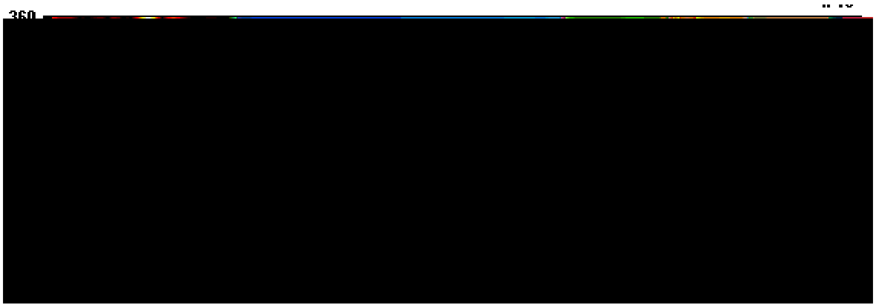

Figure 3.5: Wavelet analysis of the QNH pressure signal for September showing regular maxima approximately every hours at a scale of 120 minutes.

Two possible explanations were suggested for these pressure oscillations.

The first idea was that they result from mountain waves. These usually occur in flows perpendicular to a ridge, forming stationary waves in the lee. However, in such a flow the observation station would lie next to the ridge rather than in the wake. Parallel flows tend not to produce mountain waves since the air tends to flow around rather than over the ridge. Also, the regular occurrence of these fluctuations over very long time periods in a varying flow regime seems to make this a dubious explanation.

A second hypothesis was that they are perhaps induced by vortex shedding at the trailing edge of the mountain chain. Alternating cyclonic and anticyclonic vortices might induce local low and high pressure centers that move downstream in the wake of the obstruction, causing the observed fluctuations as they pass over the observing station. Similar oscillations were found in the wind strength but not in the wind direction.

Temperature

The temperature profiles (b)0.343079(c)0.040118(h)0.218509(e)-41.1708(i)268.688426(i)0.218509 diurnal oscillation visible in the wavelet analyses. No other structures can be observed to coincide with the storms.

Humidity

In the early autumn the humidity shows a strong diurnal cycle (dry days, humid nights) varying between 40% and 80% in August with the magnitude of observed was for the January storm which featured a long spiral arm extending southwest over Iran. However this was related to a small low pressure over northeastern Irak rather than a thermal low induced over the Caspian Sea.

Infrared data from AIRS polar orbiting satellite [24] was obtained for several of the dates of interest. None of these showed a positive thermal contrast between the lake and the near surface air that could be likened to the "'Hurricane Huron"' scenario. [14] In fact the lake surface was colder than the air over most of its area. This discards the idea that surface induced

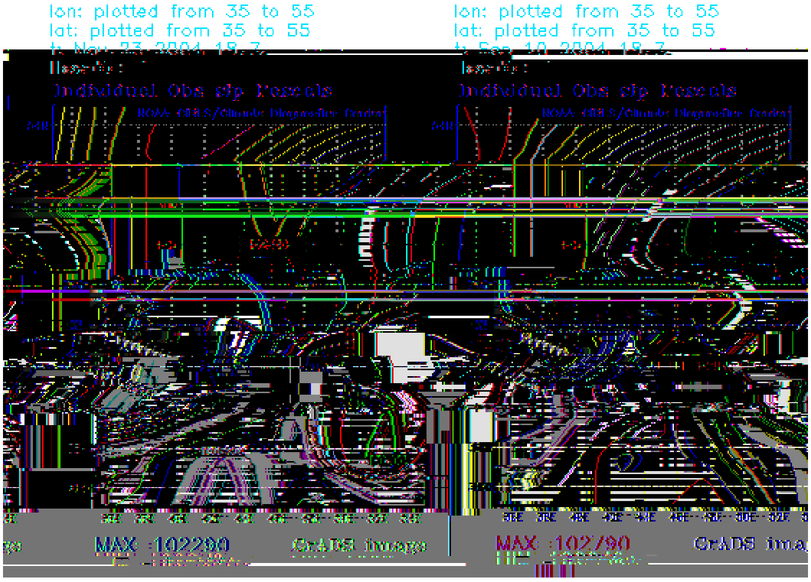

Figure 3.6: Sea level pressure plots produced by the CDC website [22]

Two distinct scenarios can be identified, both coinciding with northerly and southerly storms. Figure 3.6 depicts the case where there is a strong

where it is known that a thermal low pressure, forming over the land to the east of the lake during the day, moves across the warm lake at night causing strong winds of 20 - 30 knots in the early morning hours. [18])

Hence the storms must be induced by the synoptic flow over the region. Here we can distinguish between four cases:

1. geostrophic flow from the North producing a northerly wind storm,
2. geostrophic flow from the North producing a southerly wind storm,
3. geostrophic flow from the East producing a northerly wind storm,
4. and geostrophic flow from the East producing a southerly wind storm.

The first case seems fairly straight forward. A stable atmosphere could inhibit the air from rising over the mountain chain forcing the air around the barrier. The acceleration in the wind might then be ascribed to convergence as the air flow is diverted around the edge of a barrier in the flow. This could apply to the events on the 22 of October, 18 and 23 of November, the 11 of January and possibly the 16 of December.

The fourth case may be caused by the same mechanism in which the easterly flow may be deflected northwards by the steep slopes of the Elbruz mountains as they curve north towards Kura river valley. There a downvalley wind might block the flow from blowing up the narrow channel between the Greater and Lesser Caucasus, thereby inducing the strong southerly winds. This would account for the storms on the 7 , 18 and 24 Septmeber.

In both these cases a stable atmosphere or strong inversion would be required to inhibit vertical motion. Unfortunately no radiosonde ascents were available from upstream stations on these dates.

The Southerly storms under Northerly geostrophic flow could be explained by flow channeling as described by J. Overland in his scale analysis of ageostrophic accelerations commonly observed in marine straights. [11] This idea will be explored in the following chapter as a possible explanation for the storms on the 10 of September, 1 , 5 and 10 of December. The two summer storms on the 4 and 26 of August weakly match this case as well.

The synoptic situation on the 5 of November fits very well to the third scenario. On closer inspection however it seems that this storm may not be caused by the large scale flow seen on the synoptic charts.

It is the only storm event which shows a distinct temperature drop over the 24 hr period of the storm. An upper level trough that extends southward over the Caucasus and the very stable, dry cold air near the surface at Divnoe are suggestive of a of polar continental air mass. A weak northerly wind is recorded at midnight on the 4 . The coldest point on the temperature curve at the oil rig coincides with the strongest wind and a sharp drop (30%) in the humidity.

It seems that this storm may be better explained as a cold flow fro

Chapter 4

Southerly Storms

Figure 4.1: Frame of reference for the scale analysis. The height of the mountains lining the channel is assigned D.

$$R_L \left[\frac{du}{dt} + C'(u^2 + v^2)^{1/2} u \right] - v = -\frac{\partial p_0}{\partial x} - \frac{\partial p}{\partial x} \tag{4.5}$$

The along-channel and cross-channel Rossby numbers, R and R_L respec-

Chapter 5

A Simple Model of Mountain Blocking

3. **The friction force is proportional to the velocity - this is justified solely on the basis that it simplifies the equations.**

$$v = -U\left(1 + \frac{a^2}{r^2}\right)\sin$$

Because the ellipse is not symmetrical in all directions, we need to account for the incident angle of the freestream flow. We can now write t

inary parts within the square root by defining two variables C and D such

Chapter 6

Conclusion

Two distinct scenarios have been identified for the severe autumn and winter winds in the central Caspian Sea. These explanations are applicable to the autumn and winter months only.

Appendix A

Data Plots and Analyses

A.1 Wavelet Plots

Why Wavelets

Wavelet theory has its roots in Fourier transforms. The major di erence is that in wavelet anaylisis one compares the signal with a finite wave shape (known as the 'mother' wavelet) over a range of scales rather than an infinite wavelet transform is most applicable. [17] A popular choice is the mexican hat wavelet since it's strong localisation in time makes it idea for identifying singular events. Higher order derivatives of the gaussian wavelet can be used if one is looking for small wave groups.

Description of the Plots

The plots displayed here were generated using the 1D-continuous transform in the Matlab 'wavelet toolbox'. A mexican hat wavelet was used to analyse the signals over a range of scales from 36 - 720 minutes in intervals of 12 minutes.

The time axis is in minutes from fro a-321.298-17.9-0025(w)27.3769569(a)0.245057(s)-0.askin

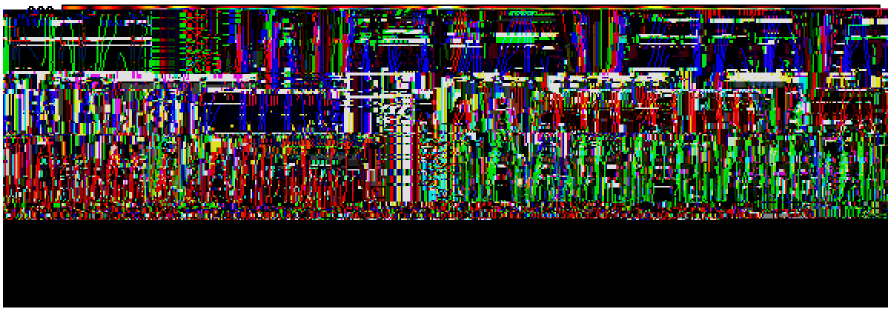

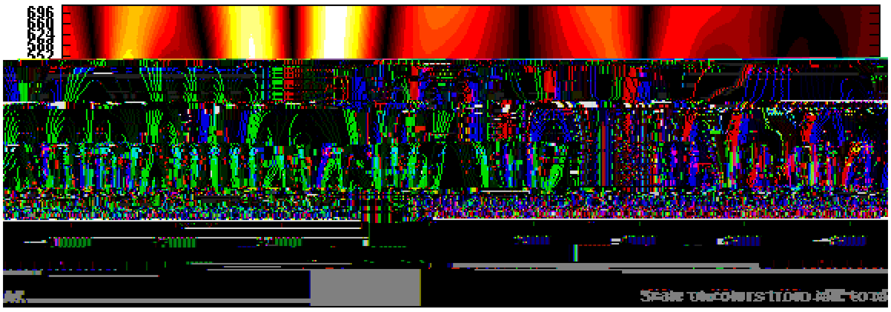

(a) Wind Speed (10 minute average)

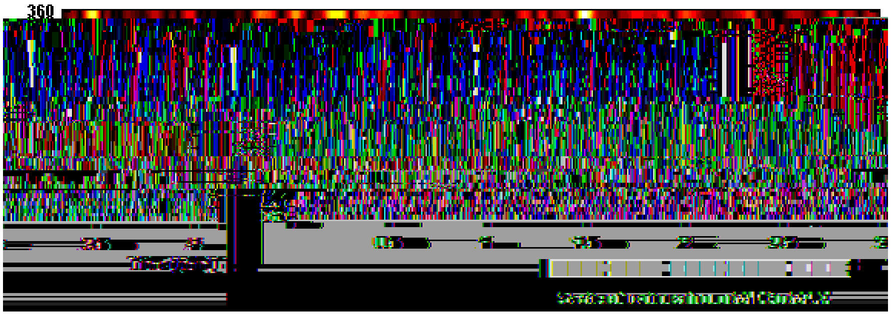

(b) QNH Pressure (10 minute average)

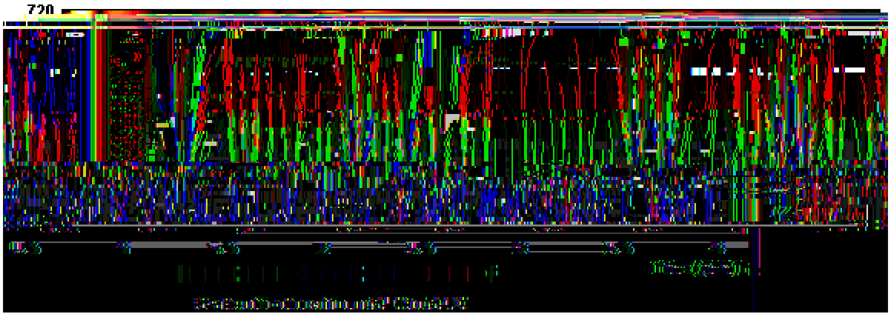

(c) Temperature (10 minute average)

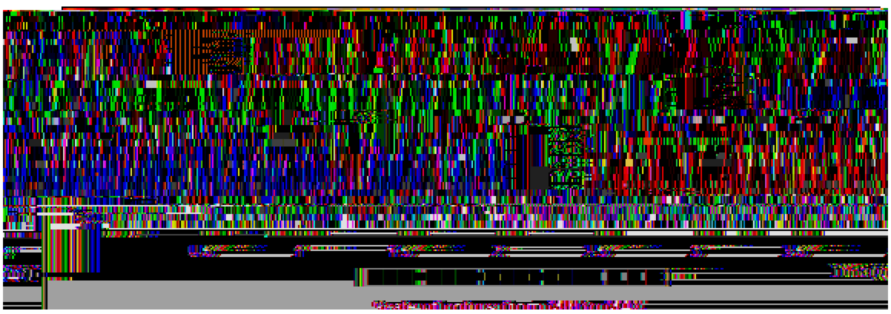

(d) Relative Humidity (10 minute average)

Figure A.2: Wavelet analysis for the month of October

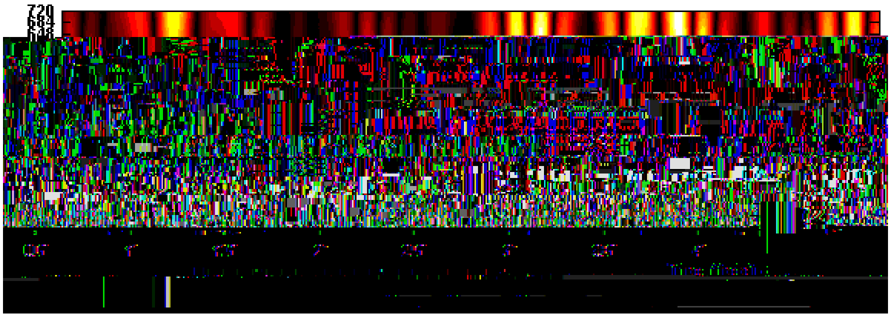

(a) Wind Speed (10 minute average)

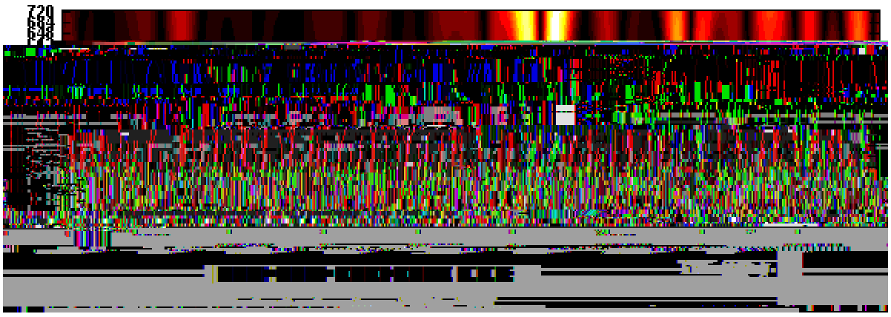

(b) QNH Pressure (10 minute average)

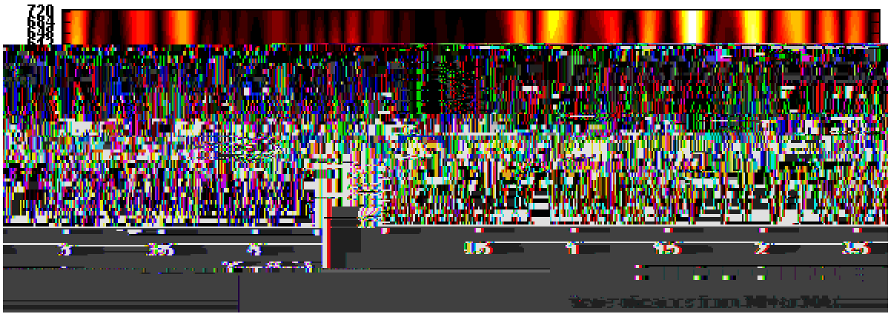

(c) Temperature (10 minute average)

(d) Relative Humidity (10 minute average)

Figure A.3: Wavelet analysis for the month of November

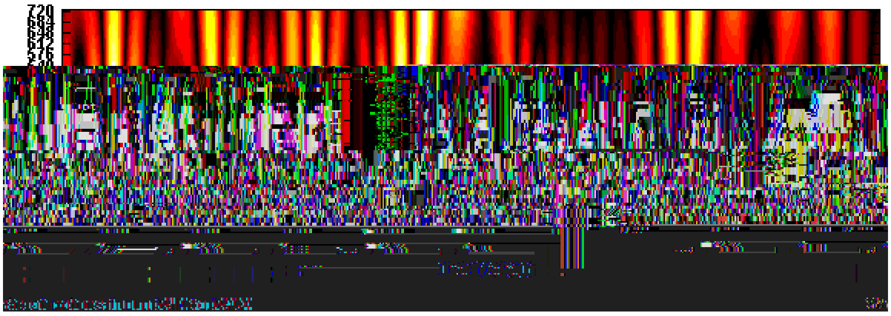

(a) Wind Speed (10 minute average)

(b) QNH Pressure (10 minute average)

(c) Temperature (10 minute average)

(d) Relative Humidity (10 minute average)

Figure A.5: Wavelet analysis for the month of January

A.2 Storm Events

The following plots are 5 day time series centered about the identified storms.

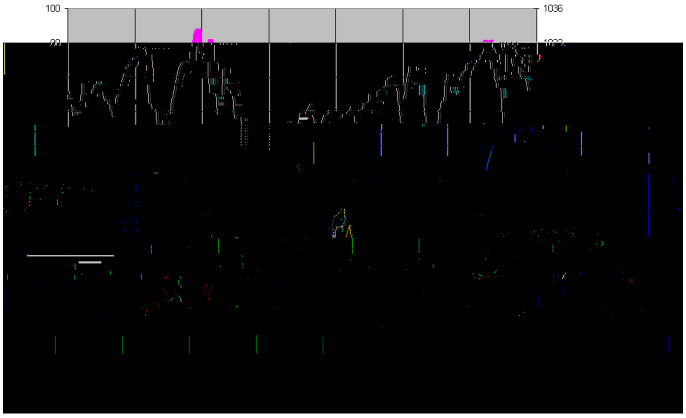

Figure A.8: Time series for the 18 of November 2004 severe gale.

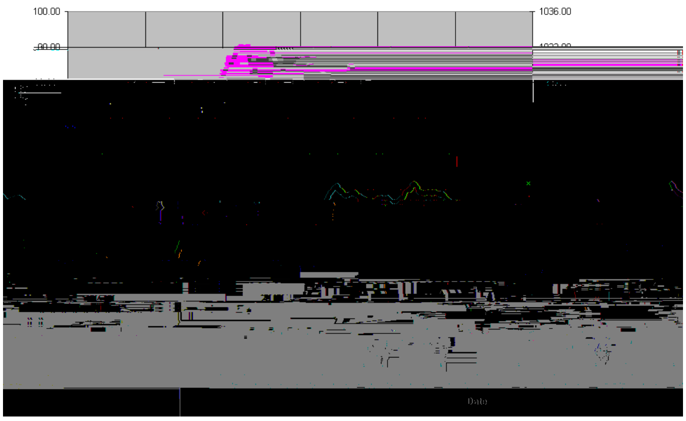

Figure A.9: Time series for the 23 of November 2004 severe gale.

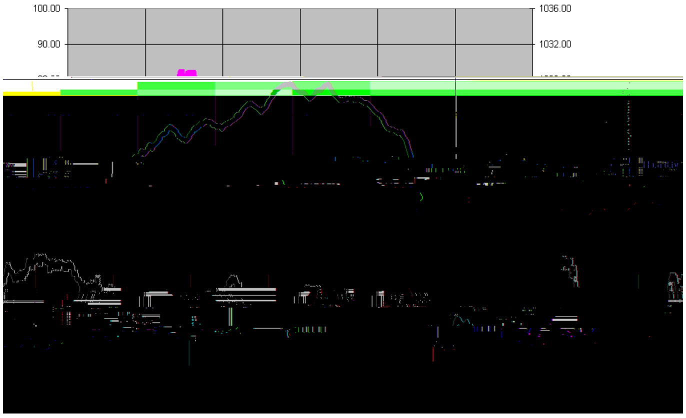

Figure A.10: Time series for the 16 of December 2004 gale.

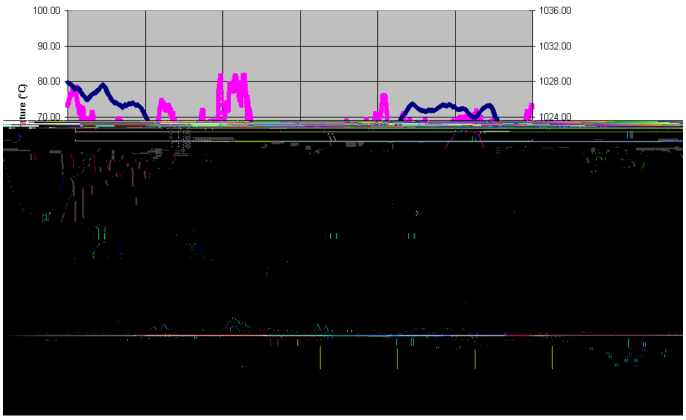

Figure A.11: Time series for the 11 of January 2005 severe gale.

Type 2. Events

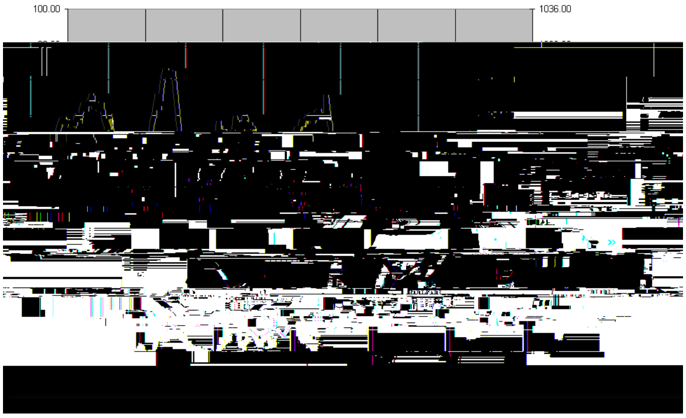

Figure A.12: Time series for the 4 of August 2004 gale.

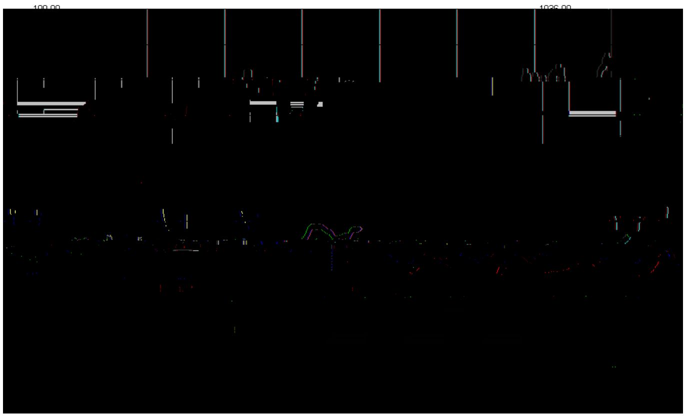

Figure A.13: Time series for the 26 of August 2004 gale.

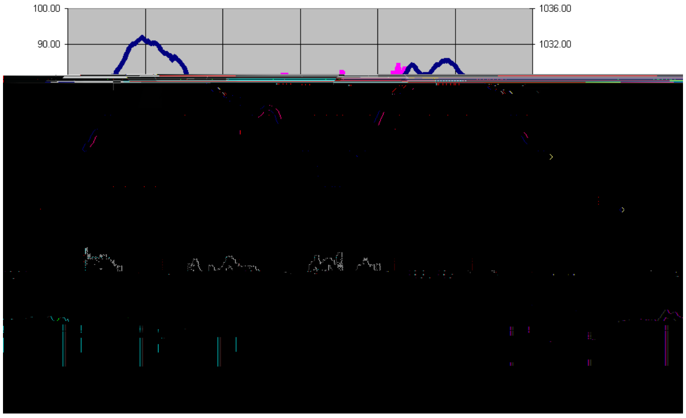

Figure A.16: Time series for the 4 of December 2004 near ani DEigure A.17: Time series

Type 4. Events

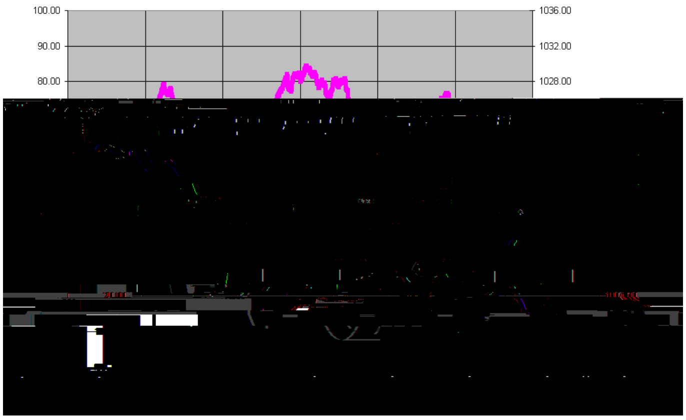

Figure A.18: Time series for the 7 of September 2004 gale.

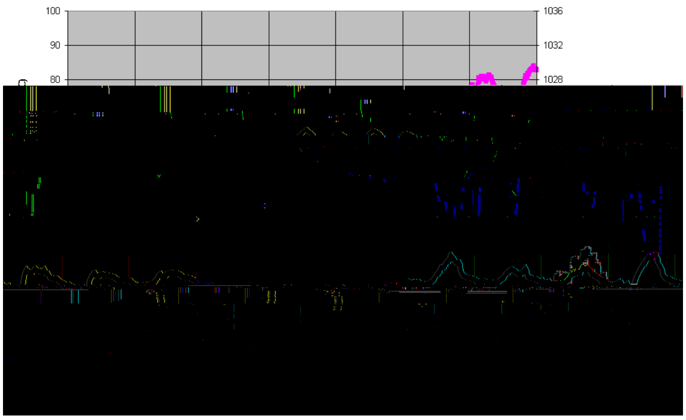

Figure A.19: Time series for the 18 of September 2004 gale.

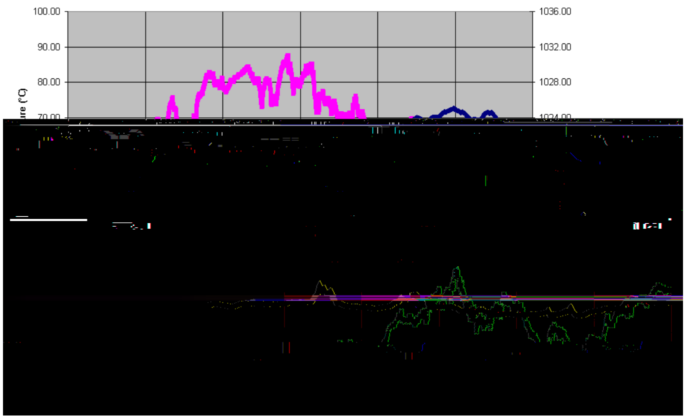

Figure A.20: Time series for the 24

[8] J. Lewalle, 1998, "Wavelets without Lemmmas: Part I of a 2-part Lecture Series on Applications of Continuous Wavelets to Data Analysis", prepared for the VKI Lecture Series April 6-8, 1998, Syracuse University, http://www.mame.syr.edu/faculty/lewalle

[20] **“Soyuz Sovetskikh Sotsialisticheshikh Respublik: uchebnaya karta”,**